

## Nonlinear Adiabatic Passage from Fermion Atoms to Boson Molecules

E. Pazy,<sup>1</sup> I. Tikhonenkov,<sup>1</sup> Y. B. Band,<sup>1</sup> M. Fleischhauer,<sup>2</sup> and A. Vardi<sup>1</sup>

<sup>1</sup>*Department of Chemistry, Ben-Gurion University of the Negev, P.O.B. 653, Beer-Sheva 84105, Israel*

<sup>2</sup>*Fachbereich Physik, Technische Universität Kaiserslautern, D67663, Kaiserslautern, Germany*

(Received 9 March 2005; published 19 October 2005)

We study the dynamics of an adiabatic sweep through a Feshbach resonance in a quantum gas of fermionic atoms. Analysis of the dynamical equations, supported by mean-field and many-body numerical results, shows that the dependence of the remaining atomic fraction  $\Gamma$  on the sweep rate  $\alpha$  varies from exponential Landau-Zener behavior for a single pair of particles to a power-law dependence for large particle number  $N$ . The power law is linear,  $\Gamma \propto \alpha$ , when the initial molecular fraction is smaller than the  $1/N$  quantum fluctuations, and  $\Gamma \propto \alpha^{1/3}$  when it is larger. Experimental data agree well with a linear dependence, but do not conclusively rule out the Landau-Zener model.

DOI: 10.1103/PhysRevLett.95.170403

PACS numbers: 03.75.Ss, 03.75.Mn, 05.30.Fk

Adiabatic sweeps across an atom-molecule Feshbach resonance have recently been used to convert degenerate fermionic atomic gases containing two different internal spin states to bosonic dimer molecules [1–4]. Formation of a molecular condensate has also been observed using both adiabatic sweeps and three-body recombination processes [5]. In this Letter we show that for adiabatic Feshbach sweeps that convert degenerate fermionic atoms to diatomic molecules, the Landau-Zener behavior for a single pair of particles [6], which is a paradigm for modeling adiabatic evolution, can be significantly altered due to many-body effects. The fraction of unconverted atoms is shown to follow a power law in the sweep rate, rather than the exponential behavior predicted by an essentially single-particle, linear Landau-Zener model [6,7]. The exact power law is determined by quantum fluctuations. En route to this result we also find that, for a ladder of atomic states filled by fermionic atoms, the atom-molecule sweep efficiency is unaffected by atomic dispersion, and all fermionic atoms can go over to molecules, in contrast to the linear Landau-Zener model. Comparison with experimental results shows good agreement but does not rule out an exponential fit.

We consider the collisionless, single bosonic mode Hamiltonian [8–14]

$$H = \sum_{\mathbf{k}, \sigma} \epsilon_{\mathbf{k}} c_{\mathbf{k}, \sigma}^{\dagger} c_{\mathbf{k}, \sigma} + \mathcal{E}(t) b_0^{\dagger} b_0 + g \left( \sum_{\mathbf{k}} c_{\mathbf{k}, \uparrow} c_{-\mathbf{k}, \downarrow} b_0^{\dagger} + \text{H.c.} \right), \quad (1)$$

where  $\epsilon_{\mathbf{k}} = \hbar^2 k^2 / 2m$  is the kinetic energy of an atom with mass  $m$ , and  $g$  is the atom-molecule coupling strength. The molecular energy  $\mathcal{E}(t) = \alpha t$  is linearly swept at a rate  $\alpha$  through resonance to induce adiabatic conversion of Fermi atoms to Bose molecules. The annihilation operators for the atoms,  $c_{\mathbf{k}, \sigma}$ , obey fermionic anticommutation relations, whereas the molecule annihilation operator  $b_0$  obeys a bosonic commutation relation.

We find that, provided that all atomic levels are swept through, the adiabatic conversion efficiency is completely insensitive to the details of the atomic dispersion. Figure 1

shows exact numerical results for the adiabatic conversion of five atom pairs into molecules, for different values of the atomic level spacing (and hence of the Fermi energy  $E_F$ ). It is evident that, while the exact dynamics depends on  $E_F$ , levels are sequentially crossed, leading to the same final efficiency regardless of the atomic motional time scale. In particular, in the limit as  $\alpha \rightarrow 0$ , it is possible to convert *all* atom pairs into molecules. This is a unique feature of the nonlinear parametric coupling between atoms and molecules, which should be contrasted with a marginal conversion efficiency expected for linear coupling. Since the exact energies  $\epsilon_{\mathbf{k}}$  do not affect the final fraction of molecules, we use a degenerate model [12–14] with  $\epsilon_{\mathbf{k}} = \epsilon$  for all  $\mathbf{k}$ . In the spirit of Refs. [13,15], we define the operators:

$$J_- = \frac{b_0^{\dagger} \sum_{\mathbf{k}} c_{\mathbf{k}, \uparrow} c_{-\mathbf{k}, \downarrow}}{(N/2)^{3/2}}, \quad J_+ = \frac{\sum_{\mathbf{k}} c_{-\mathbf{k}, \downarrow}^{\dagger} c_{\mathbf{k}, \uparrow}^{\dagger} b_0}{(N/2)^{3/2}}, \quad (2)$$

$$J_z = \frac{\sum_{\mathbf{k}, \sigma} c_{\mathbf{k}, \sigma}^{\dagger} c_{\mathbf{k}, \sigma} - 2b_0^{\dagger} b_0}{N},$$

where  $N = 2b_0^{\dagger} b_0 + \sum_{\mathbf{k}, \sigma} c_{\mathbf{k}, \sigma}^{\dagger} c_{\mathbf{k}, \sigma}$  is the conserved total

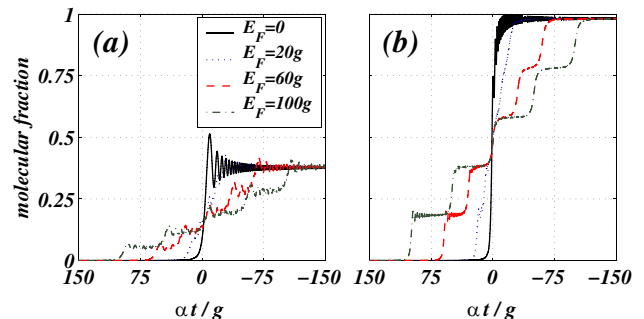


FIG. 1 (color online). Many-body collective dynamics of adiabatic passage from a fermionic atomic gas into a molecular BEC for five pairs of fermionic atoms. (a) Sweep rate  $\alpha = 2g^2N$ . (b) Sweep rate  $\alpha = g^2N/4$ . Overall efficiency is independent of atomic dispersion in both (a) and (b).

number of particles. It is important to note that  $J_-, J_+, J_z$  do not span  $SU(2)$  as  $[J_+, J_-]$  is a quadratic polynomial in  $J_z$ . We also define  $J_x = J_+ + J_-$  and  $J_y = -i(J_+ - J_-)$ . Up to a  $c$ -number term, Hamiltonian (1) takes the form

$$H = \frac{N}{2} \left( \Delta(t) J_z + g \sqrt{\frac{N}{2}} J_x \right), \quad (3)$$

where  $\Delta(t) = 2\epsilon - \mathcal{E}(t)$ . Defining a rescaled time  $\tau = \sqrt{N}gt$ , we obtain the Heisenberg equations of motion for the association of a quantum-degenerate gas of fermions,

$$\begin{aligned} \frac{d}{d\tau} J_x &= \delta(\tau) J_y \\ \frac{d}{d\tau} J_y &= -\delta(\tau) J_x + \frac{3\sqrt{2}}{4} (J_z - 1) \left( J_z + \frac{1}{3} \right) - \frac{\sqrt{2}}{N} (1 + J_z), \\ \frac{d}{d\tau} J_z &= \sqrt{2} J_y, \end{aligned} \quad (4)$$

which depend on the single parameter  $\delta(\tau) = \Delta(t)/\sqrt{N}g = (\alpha/g^2N)\tau$ . We note parenthetically that precisely the same set of equations, with  $J_z \rightarrow -J_z$  and  $g \rightarrow g/2$ , is obtained for a two-mode atom-molecule Bose-Einstein condensate (BEC) [15], highlighting a mapping between the two systems [12–14].

We first consider the mean-field limit of Eqs. (4), replacing  $J_x, J_y$ , and  $J_z$  by their expectation values  $u, v$ , and  $w$  which correspond to the real and imaginary parts of the atom-molecule coherence and the atom-molecule population imbalance, respectively, and omitting the quantum-noise term  $\sqrt{2}(1 + J_z)/N$ . In this limit, the equations depict the motion of a generalized Bloch vector on a two-dimensional surface, determined by the conservation law,

$$u^2 + v^2 = \frac{1}{2}(w-1)^2(w+1). \quad (5)$$

Hamiltonian (3) is then replaced by the classical form

$$H(w, \theta; \Delta) = \frac{gN^{3/2}}{2} \left( \delta w + \sqrt{(1+w)(1-w^2)} \cos\theta \right), \quad (6)$$

with  $\theta = \arctan(v/u)$ .

To study the atom-molecule adiabatic passage, we closely follow the method of Ref. [16]. The eigenvalues of the atom-molecule system at any given value of  $\delta$  correspond to the fixed points  $(u_0, v_0, w_0)$  of the classical Hamiltonian (6) or the mean-field limit of Eqs. (4):

$$v_0 = 0, \quad \frac{\sqrt{2}}{4}(w_0 - 1)(3w_0 + 1) = \delta u_0. \quad (7)$$

The number of fixed points depends on the parameter  $\delta$ . The point  $u_0 = v_0 = 0, w_0 = 1$  is stationary for any value of  $\delta$ . Using Eqs. (5) and (7), other fixed points satisfy

$$\frac{(3w_0 + 1)^2}{4(w_0 + 1)} = \delta^2. \quad (8)$$

In Fig. 2 we plot phase-space trajectories, corresponding to equal-energy contours of Hamiltonian (6), for different values of  $\delta$ . As expected from (6), the plots have the symmetry  $(w, \theta; \delta) \leftrightarrow (w, \theta + \pi; -\delta)$ . For sufficiently large detuning,  $|\delta| > \sqrt{2}$ , Eq. (8) has only one solution in the range  $-1 \leq w_0 \leq 1$ . Therefore, there are only two (elliptic) fixed points, denoted by a red circle corresponding to the solution of Eq. (8) and a blue square at  $(0, 0, 1)$ . As the detuning is changed, one of these fixed points (red circle) smoothly moves from all molecules towards the atomic mode. At detuning  $\delta = -\sqrt{2}$  a homoclinic orbit appears through the point  $(0, 0, 1)$  which bifurcates into an unstable (hyperbolic) fixed point (black star) remaining on the atomic mode, and an elliptic fixed point (blue square) which starts moving towards the molecular mode. Consequently, in the regime  $|\delta| < \sqrt{2}$  there are two elliptic fixed points and one hyperbolic fixed point, corresponding to the unstable all-atoms mode. Another crossing occurs at  $\delta = \sqrt{2}$  when the fixed point that started near the molecular mode (red circle) coalesces with the all-atoms mode (black star).

The frequency of small periodic orbits around the fixed points,  $\Omega_0$ , is found by linearization of the dynamical Eqs. (4) about  $(u_0, v_0, w_0)$  and using (8) to obtain

$$\frac{\Omega_0}{g\sqrt{N}} = \sqrt{\delta^2 + (1 - 3w_0)} = \sqrt{\frac{(1 - w_0)(3w_0 + 5)}{4(w_0 + 1)}}. \quad (9)$$

Hence, for  $|\delta| < \sqrt{2}$  the period of the homoclinic trajectory beginning at  $(0, 0, 1)$  diverges.

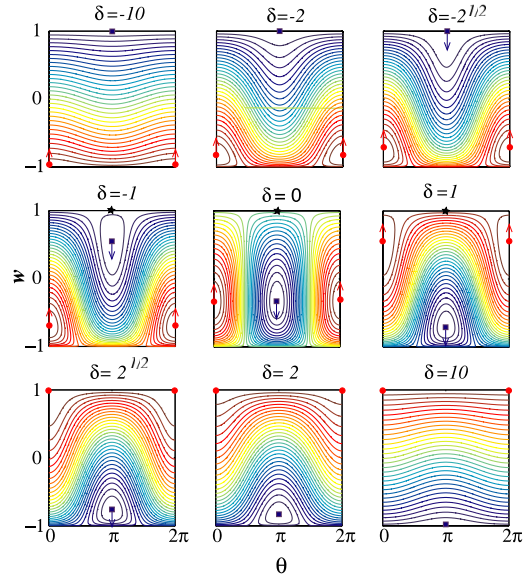


FIG. 2 (color online). Equal-energy contours of Hamiltonian (6) plotted as a function of  $w$  and  $\theta$  for different detunings  $\delta$ .  $w = 1$  is all atoms and  $w = -1$  is all molecules. The various fixed points corresponding to adiabatic eigenvectors are marked by (blue) squares, (red) circles, and (black) stars.

Transforming  $w, \theta$  into action-angle variables  $I, \phi$ , the nonadiabatic probability  $\Gamma$  at any finite sweep rate  $\alpha$  is related to the action  $I$  accumulated during the sweep [6,16,17],

$$\Gamma^2 = \frac{\Delta I}{2} = \frac{1}{2} \int_{-\infty}^{\infty} R(I, \phi) \dot{\Delta} \frac{d\phi}{\dot{\phi}}, \quad (10)$$

where  $R(I, \phi)$  is related to the generating function of the canonical transformation  $w, \theta \rightarrow I, \phi$ . We note that, unlike the linear [6] or Josephson [16,17] case, where the tunneling probability is linearly proportional to the action increment  $\Delta I$ , our choice of variables (2) causes the atomic population at the end of the sweep (and, hence,  $\Gamma$ ) to be proportional to the *square root* of  $\Delta I$  [since  $u^2(t_f) + v^2(t_f) \propto |\sum_{\mathbf{k}, \sigma} n_{\mathbf{k}, \sigma}(t_f)|^2$ , where  $n_{\mathbf{k}, \sigma}(t_f)$  is the population in state  $|\mathbf{k}, \sigma\rangle$  at the final time  $t_f$ ]. Equation (10) depicts the familiar rule that in order to attain adiabaticity, the rate of change of the adiabatic fixed points through the variation of the adiabatic parameter  $\Delta$ ,  $R(I, \phi)\dot{\Delta}$ , should be slow with respect to the characteristic precession frequency  $\dot{\phi} = \Omega_0$  about these stationary vectors. For an adiabatic process where  $\dot{\Delta}/\dot{\phi} \rightarrow 0$ , the action (which is proportional to the surface area enclosed within the periodic orbit) is an adiabatic invariant, so a zero-action elliptic fixed point evolves into a similar point trajectory. Action is accumulated mainly in the vicinity of singularities where  $\dot{\phi} = \Omega_0 \rightarrow 0$ . For linear adiabatic passage [6], such singular points lie exclusively off the real axis, leading to exponential Landau-Zener transition probabilities. However, when nonlinearities are dominant, as in the Mott-insulating Josephson case [16,17] and our case, there are real singularities, leading to power-law dependence of the transfer efficiency on the sweep rate.

It is clear from (9) that, for atom-molecule conversion, a real singularity of the integrand in (10) exists at  $w_0 = 1$ , where the frequency vanishes as  $\Omega_0 \approx g\sqrt{N(1-w_0)}$ . Thus, most of the nonadiabatic correction is accumulated in the vicinity of this point (all atoms for fermions and all molecules for bosons). Differentiating Eq. (8) with respect to  $t$ , we find that the response of the fixed-point velocity to a linear sweep rate is

$$\dot{w}_0 = \frac{4\alpha}{g\sqrt{N}} \frac{(w_0 + 1)^{3/2}}{3w_0 + 5}. \quad (11)$$

Having found  $\dot{w}_0$ , we can now find the action-angle variable  $\phi$  in terms of  $w_0$ :  $\phi = \int \dot{\phi} dt = \int \Omega_0 \frac{dw_0}{\dot{w}_0}$ . In the vicinity of the singularity we have  $\Omega_0 \approx g\sqrt{N(1-w_0)}$  and  $\dot{w}_0 \approx \sqrt{2}\alpha/g\sqrt{N}$ , resulting in

$$\phi = \frac{g^2 N}{\alpha} \frac{\sqrt{2}}{3} (1-w_0)^{3/2}. \quad (12)$$

Using Eq. (12), we finally find that near the singularity,  $\dot{\phi} = \Omega_0 \approx g\sqrt{N(1-w_0)}$  is given in terms of  $\phi$  as

$$\dot{\phi} = \left(3\sqrt{\frac{N}{2}}g\alpha\right)^{1/3} \phi^{1/3}. \quad (13)$$

Substituting (13) and  $\dot{\Delta} = \alpha$  into Eq. (10) we find that the nonadiabatic correction depends on  $\alpha$  as

$$\Gamma \propto \alpha^{1/3}. \quad (14)$$

So far, we have neglected the effect of quantum fluctuations, which are partially accounted for by the source term  $(\sqrt{2}/N)(1 + J_z)$  in Eqs. (4). As a result, we found that  $\dot{w}_0$  does not vanish as  $w_0$  approaches 1. Consequently, the remaining atomic population is expected to scale as the cubic root of the sweep rate if the initial average molecular fraction is larger than the quantum noise. However, starting purely with fermion atoms (or with molecules made of bosonic atoms), fluctuations will initially dominate the conversion process. Equation (8) should then be replaced by

$$\delta = \frac{2}{\sqrt{w_0 + 1}} \left( \frac{3w_0 + 1}{4} - \frac{w_0 + 1}{N(w_0 - 1)} \right), \quad (15)$$

demonstrating that our previous treatment around  $w_0 = 1$  is only valid provided that  $|w_0(t_i) - 1| \gg 1/N$ . For smaller initial molecular population, Eq. (11) should be replaced by

$$\dot{w}_0 = \frac{\alpha}{g\sqrt{N}} \left/ \left[ \frac{3w_0 + 5}{4(w_0 + 1)^{3/2}} + \frac{w_0 + 3}{N(w_0 + 1)^{1/2}(w_0 - 1)^2} \right] \right., \quad (16)$$

Hence, in the vicinity of  $w_0 = 1$  the eigenvector velocity in the  $w$  direction vanishes as  $\dot{w}_0 = (\sqrt{N}\alpha/g\sqrt{8})(w_0 - 1)^2$ . The characteristic frequency  $\dot{\phi}$  is now proportional to  $(\alpha\phi)^{-1}$  instead of Eq. (13) so that  $\Delta I \propto \alpha^2$ , and [18,19]

$$\Gamma \propto \alpha. \quad (17)$$

Equations (17) and (14) constitute the main results of this work. We predict that the remnant atomic fraction in adiabatic Feshbach sweep experiments will scale as a power law with sweep rate due to the curve crossing in the nonlinear case. The dependence is expected to be linear if the initial molecular population is below the quantum-noise level [i.e., when  $1 - w_0(t_i) \ll 1/N$ ], and cubic root when fluctuations can be neglected [i.e., for  $1 - w_0(t_i) \gg 1/N$ ]. We note that a similar linear dependence was predicted for adiabatic passage from bosonic atoms into a molecular BEC [18].

The analytical predictions illustrated above are confirmed by numerical simulations. Figure 3 shows  $\Gamma$  versus dimensionless inverse sweep rate  $\frac{g^2}{\alpha N}$ . Exact many-body numerical calculations for particle numbers in the range  $2 \leq N \leq 800$ , carried out using the methodology of [12], are compared with a mean-field curve (solid green line), computed numerically from the mean-field limit of Eqs. (4). The log-log plot highlights the power-law depen-

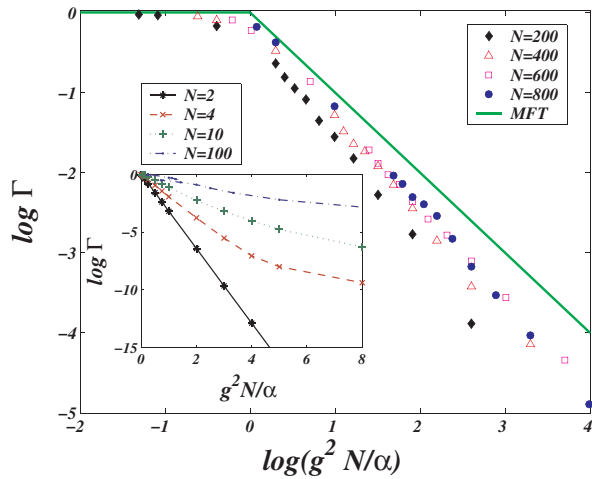


FIG. 3 (color online). Many-body calculations for the fraction of remnant atoms,  $\Gamma$ , versus dimensionless inverse sweep rate for various particle numbers in the range  $N = 2$  to 800. The many-body results for a large number of particles converge to the mean-field results (solid green line) of Fig. 4.

dence, obtained in the slow ramp regime  $\alpha < g^2N$ , whereas the log-linear inset plot demonstrates exponential behavior (for  $N = 2$ ). For a single pair of particles,  $N = 2$ , the quantum association problem is formally identical to the linear Landau-Zener paradigm, leading to an exponential dependence of  $\Gamma$  on sweep rate. However, as the number of particles increases, many-body effects come into play, and there is a smooth transition to a power-law

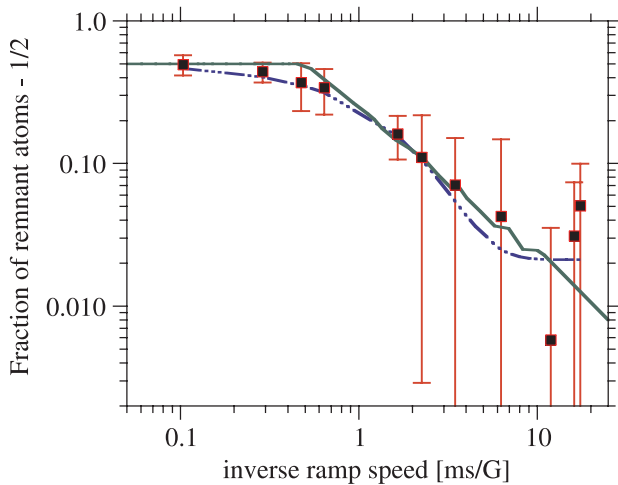


FIG. 4 (color online). Fraction of remnant atoms,  $\Gamma$ , versus inverse ramp speed  $1/\dot{B}$  across the 543 G resonance of  ${}^6\text{Li}$ . The experimental data (black squares) of [2], which saturate at a remnant of  $1/2$  [20], and the mean-field calculations obey a linear dependence on sweep rate beyond  $0.5$  ms/G. The  $g^2/\alpha N$  is multiplied by  $0.5$  ms/G to scale the abscissa for the calculated results. Also shown as a dashed line is the best exponential fit to the data,  $\Gamma = 0.479 \exp(-\alpha/1.3) + 0.521$ .

behavior in the slow ramp regime  $\alpha < g^2N$ . We note that this is precisely the regime where Eq. (10) can be used to estimate  $\Delta I$  and  $\Gamma$  [6]. The many-body calculations converge to the mean-field limit, corresponding to a linear dependence of  $\Gamma$  on  $\alpha$ , as predicted in Eq. (17).

In Fig. 4, we compare our mean-field numerical calculation with the experimental data of Ref. [2]. The theory agrees very well with the experiment. However, since an equally good exponential fit can be found [2], as shown in Fig. 4 (dashed line), current experimental data does not serve to determine which of the alternative theories is more appropriate. We have obtained similar agreement with the experimental data of Ref. [1], but data scatter and error bars are again too large to conclusively resolve power laws from exponentials. Further precise experimental data for slow ramp speeds and different particle numbers will be required to verify or to refute our theory.

This work was supported in part by grants from the U.S.-Israel Binational Science Foundation (Grants No. 2002214 and No. 2002147), the Minerva Foundation through a grant for a Minerva Junior Research Group, the Israel Science Foundation for a Center of Excellence (Grant No. 8006/03), and the German Federal Ministry of Education and Research (BMBF) through the DIP project.

- 
- [1] C. A. Regal *et al.*, Nature (London) **424**, 47 (2003).
  - [2] K. E. Strecker *et al.*, Phys. Rev. Lett. **91**, 080406 (2003).
  - [3] J. Cubizolles *et al.*, Phys. Rev. Lett. **91**, 240401 (2003).
  - [4] E. Hodby *et al.*, Phys. Rev. Lett. **94**, 120402 (2005).
  - [5] M. Greiner *et al.*, Nature (London) **426**, 537 (2003); S. Jochim *et al.*, Science **302**, 2101 (2003); M. W. Zwierlein *et al.*, Phys. Rev. Lett. **91**, 250401 (2003).
  - [6] L. D. Landau, Phys. Z. Sowjetunion **2**, 46 (1932); G. Zener, Proc. R. Soc. A **137**, 696 (1932); L. D. Landau and E. M. Lifshitz, *Mechanics* (Pergamon, Oxford, 1976), Sec. 51.
  - [7] F. H. Mies *et al.*, Phys. Rev. A **61**, 022721 (2000); K. Góral *et al.*, J. Phys. B **37**, 3457 (2004); J. Chwedeńczuk *et al.*, Phys. Rev. Lett. **93**, 260403 (2004).
  - [8] J. Javanainen *et al.*, Phys. Rev. Lett. **92**, 200402 (2004).
  - [9] R. A. Barankov and L. S. Levitov, Phys. Rev. Lett. **93**, 130403 (2004).
  - [10] A. V. Andreev *et al.*, Phys. Rev. Lett. **93**, 130402 (2004).
  - [11] J. Dukelsky *et al.*, Phys. Rev. Lett. **93**, 050403 (2004).
  - [12] I. Tikhonenkov and A. Vardi, cond-mat/0407424.
  - [13] T. Miyakawa and P. Meystre, Phys. Rev. A **71**, 033624 (2005).
  - [14] M. Mackie and O. Dannenberg, physics/0412048.
  - [15] A. Vardi *et al.*, Phys. Rev. A **64**, 063611 (2001).
  - [16] J. Liu *et al.*, Phys. Rev. A **66**, 023404 (2002).
  - [17] O. Zobay and B. M. Garraway, Phys. Rev. A **61**, 033603 (2000).
  - [18] A. Ishkhanyan *et al.*, Phys. Rev. A **69**, 043612 (2004).
  - [19] E. Altman and A. Vishwanath, Phys. Rev. Lett. **95**, 110404 (2005).
  - [20] E. Pazy *et al.*, Phys. Rev. Lett. **93**, 120409 (2004).